Journal of Alloys and Compounds 520 (2012) 83–88

Contents lists available at SciVerse ScienceDirect

Journal of Alloys and Compounds

journal homepage: www.elsevier.com/locate/jallcom

Ag doped ZnTe films prepared by closed space sublimation and an ion exchange process

Akram K.S. Aqili[a,*], Ahmad J. Saleh[a], Zulfiqar Ali[b], S. Al-Omari[a]

[a] Department of Physics, The Hashemite University, Zarqa, Jordan
[b] Optics Laboratories, Islamabad, Pakistan

ARTICLE INFO

Article history:
Received 22 August 2011
Received in revised form
18 December 2011
Accepted 19 December 2011
Available online 9 January 2012

PACS:
73.61.Ga
78.66.Fd
71.20.Nr
73.61.Ga
61.72 ;uj

Keywords:
Thermal coating
ZnTe thin films
Optical
Electrical

ABSTRACT

ZnTe thin films were deposited by closed space sublimation (CSS) technique on amorphous glass substrate. The deposited films were immersed in $AgNO_3$ solution for different time periods, then heated in vacuum. The resistivity of the film, immersed for 30 min, was reduced by less than six orders of magnitudes. The films structures were characterized by X-ray diffraction (XRD). Atomic force microscope (AFM) was used to detect the surface morphology of the films. The films thickness, the optical properties, such as refractive index, absorption coefficient and the optical band gap were determined from transmittance spectra in the wavelength range of 400–2500 nm. The dark electrical conductivities of the films were studied as function of temperature to determine the conductivity activation energy.

1. Introduction

Among II–VI compound semiconductors zinc telluride (ZnTe) is very attractive for optoelectronic device applications in the green spectral range, due to its direct band gap of ~2.26 eV [1–4].

ZnTe thin films were prepared by several techniques including pulsed laser deposition [1], sputtering [5], electron beam [6], electro-deposition [7], isothermal closed space sublimation [8], SILAR method [9], brush plated [2], thermal evaporation [10–12] and CSS [13]. On the other hand, ion exchange process was recently utilized for doping of ZnTe and other II–VI semiconductors by Cu, Ag and In [10,13–22] due to the simplicity and low cost of the method.

One of the most important application of ZnTe is high efficiency stable electrical back contacts for CdTe based solar cells [2,4]. For that low resistive p-type ZnTe is required. Ag as group I element acts as acceptor dopant for II–VI semiconductors [23], which lead to increase in the electrical conductivity of ZnTe.

In this work we deposited ZnTe films by CSS method, which was more common for deposition of CdTe based solar cells, and Ag doping of the films was achieved by an ion exchange process. In this regard the electrical properties of the films were studied. Furthermore the optical, structural and surface morphology of the films were also studied due to its importance in the application of ZnTe in optical devices.

2. Experimental methods

High purity (99.99%) ZnTe fine powder was used as a source material for films deposition on water-white glass substrates (2.5 cm × 5 cm). Before deposition, the substrate was cleaned by diluted H_2SO_4 solution, then rinsed by distilled water and I.P.A and then dried by dry nitrogen gas. Source material (0.1 g of ZnTe) was put in the graphite boat, to be heated by 500 W quartz lamp. The source and substrate heaters (quartz lamps) were connected to the main through two separate triacs. The gates of the triacs were connected to temperature controllers. The, k-type, thermocouples of the temperature controllers were inserted into the source graphite boat and the graphite substrate supporter. The CSS system, used in our experiment, is shown in Fig. 1. Substrate was fixed at a

* Corresponding author.
E-mail address: akramaq@hu.edu.jo (A.K.S. Aqili).

0925-8388/$ – see front matter © 2012 Elsevier B.V. All rights reserved.
doi:10.1016/j.jallcom.2011.12.094

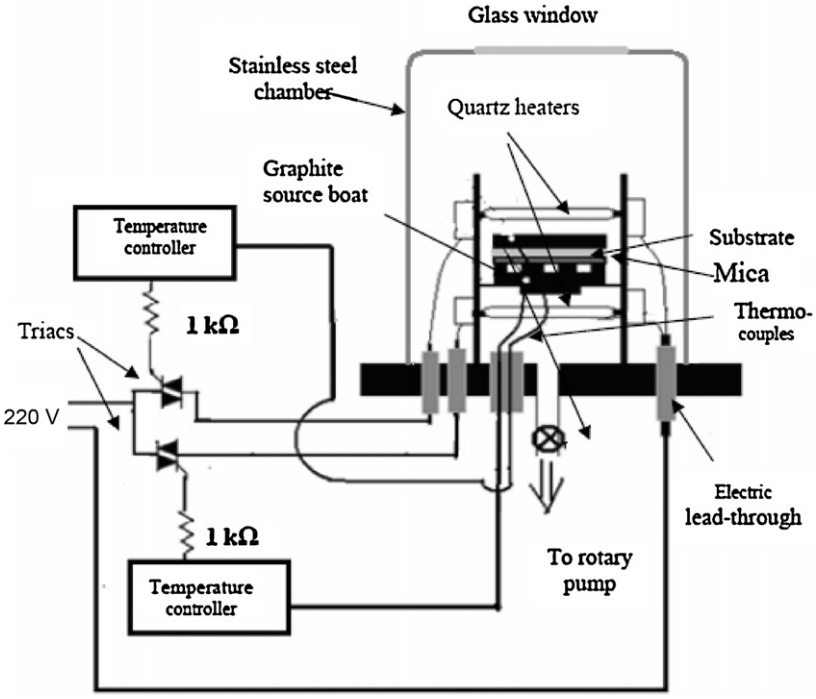

Fig. 1. Block diagram of coating system, used for deposition of the films.

distance of about 10 mm from the source of material. The chamber was closed and evacuated, by the help of rotary pump, to $\sim 1 \times 10^{-2}$ mbar. The substrate and source temperatures were kept at 400 °C and 600 °C, respectively. The time of evaporation was 10 min. The chamber was evacuated for 30 min before starting the source and substrate heating. After deposition, the source heater was turned off, while the substrate remains at the deposition temperature for 30 min. This was to allow the source temperature to cool down, avoiding further deposition at lower substrate temperature. The film remains under vacuum till source temperature reduced to below 100 °C, to avoid the oxidation of the film.

Numbers of films were prepared with similar deposition parameters to study the effect of post treating in $AgNO_3$ solution. The solution contained 1 g of $AgNO_3$ in 1 l of distilled H_2O. The solution was kept at 60 ± 2 °C. The films were immersed for different time, as listed in Table 1. After immersion the films were cleaned in distilled water and dried by nitrogen gas. Next step was heating the immersed films, in vacuum of $\sim 10^{-2}$ mbar, at 400 °C for 1 h to ensure the diffusion of Ag into the entire film [10]. Ion exchange process occurs on the films surface, i.e. Ag layer formed above the ZnTe film. So heating the films, at high temperature, cause diffusion of Ag atoms in the entire film. Further studying the Ag doping of ZnTe films, not the properties of Ag layer on ZnTe films.

X-ray diffraction (XRD) patterns, using Cu-Kα radiation, were used to study the structure of the films. The transmission spectra in the range 400–2500 nm were recorded by PerkinElmer, Lambda19, UV–vis–NIR spectrophotometer with UV-WinLab software. The dark electrical DC conductivity, of cut pieces of the films with evaporated Au contact, according to Van der Pauw geometry, was measured as a function of temperature (30–200 °C). The morphology of the films was analyzed by using atomic force microscope (AFM). The composition of the films were detected using electron micro-probe analyzer (EMPA) attached to scanning electron microscope.

Table 1
Immersion time and Ag ratio in the films.

Film number	Immersion time (min)	Ag ratio (atm.%)
Z0 (as- deposited)	0	0
Z1	1	1.7
Z5	5	8.0
Z30	30	12.9

3. Results and discussions

3.1. Structure and morphology studies

Fig. 2 shows the XRD pattern for as- deposited and immersed films. All the peaks in XRD pattern of as- deposited film was referred to Ag cubic structure of ZnTe, which is the most dominant structure for ZnTe [10,13]. The most dominant peaks in the XRD patterns are corresponding to (1 1 1), (2 2 0) and (3 1 1) direction, other low intensity peaks corresponding to (2 0 0), (2 2 2), (4 0 0), (3 3 1), (4 2 0), (4 2 2) and (5 1 1) were also observed. No peaks related to Ag or Ag compounds were observed in the XRD pattern of the films immersed in $AgNO_3$ solution for short time (i.e. ≤5 min). This could be due to small amount of Ag in the films, which is below the detection limit [10,15]. However peaks related to monoclinic structure of Ag_2Te appears in the films, which is immersed for longer time (i.e. 30 min).

Due to an ion exchange in $AgNO_3$ solution different ways of Ag incorporation in ZnTe could be possible. Substitution of Zn^{2+} by Ag^{1+} since the following interaction is possible [24].

$$Zn + 2(Ag^{+} + e) \rightarrow Zn^{2+} + 2e + 2(Ag),$$

or incorporation of Ag as interstitial in ZnTe or formation of Ag_2Te.

AFM was used to assess the surface quality of the films. Surface morphology of the films deposited at 400 °C substrate temperatures and immersed in Ag NO_3 solution, for different periods of time, and followed by heat treatment are shown in Fig. 3. The average surface roughness observed by AFM were in the range 16–18 nm, while the average grains size were ~0.3 μm and almost the same for all the

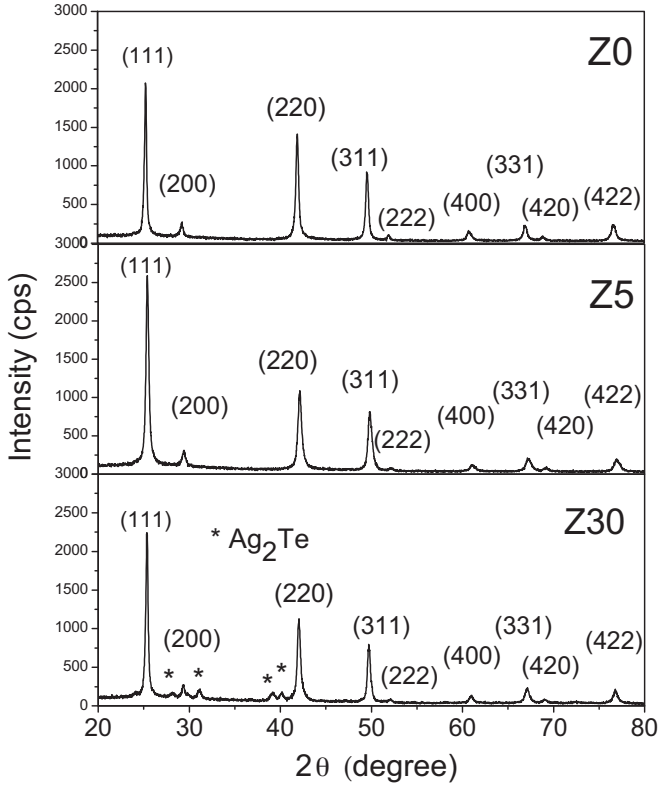

Fig. 2. XRD pattern of heated the films.

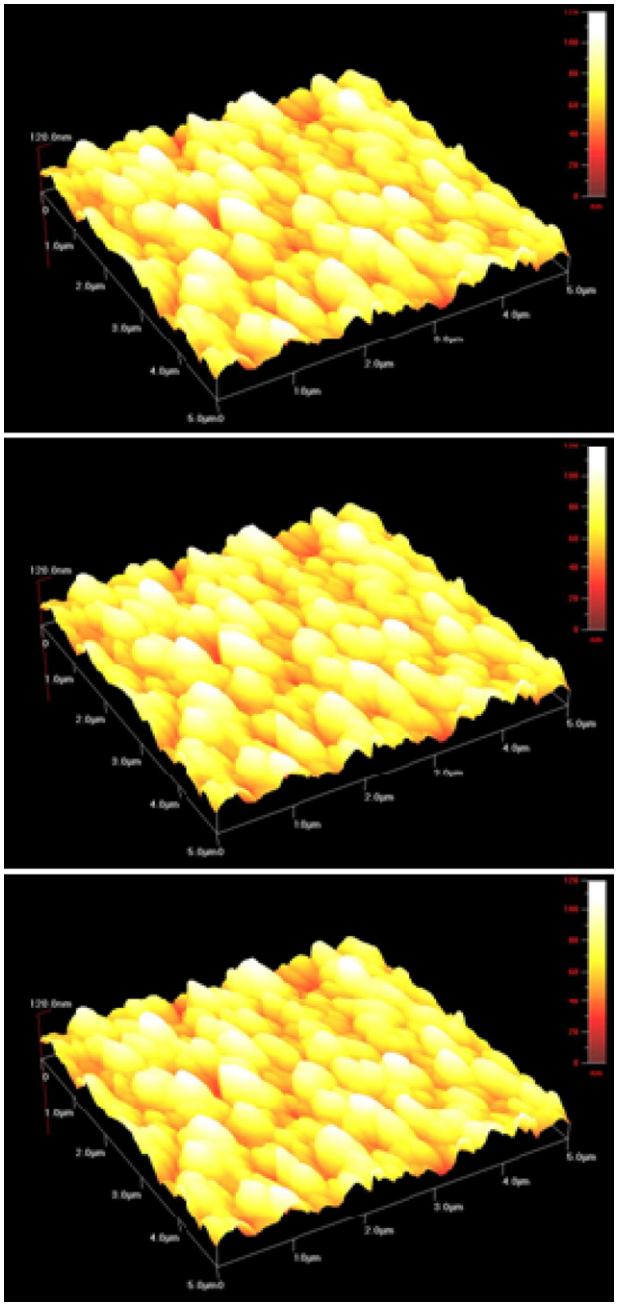

Fig. 3. AFM image of heated Z0 (up), Z5 (middle) and Z30 (down).

films. This indicates that the structure and the films morphology are more depending on the films deposition parameters. It is well known that deposition parameters such as substrate temperature, deposition rate and vacuum have great influence on the films structure and roughness. In our case these parameter were the same for all films. And the only different parameter was post treatment in $AgNO_3$ solution.

The Ag ratio (atom %) in the films (EMPA result) versus the immersion time in AgNO3 solution are listed in Table 1. It shows a non linear behavior i.e. the speed of the silver adsorbance at the film decreases with time and this result is observed for other II–VI semiconductors [10,13,14,16,17,19–22] and this was explained by the fact that ion exchange process takes place on the film surface, which was exposed to the liquid. However, the concentration of silver in these films is much higher than the films prepared by two-source evaporation [10] and immersed in $AgNO_3$ solution. The most probable explanation is the comparative surface roughness of the films (i.e. more area is exposed to the solution).

3.2. Optical analysis

The thickness and refractive index of the films were calculated by fitting the transmission data to the following equation [10,11,25]

$$T = \frac{Ax}{B - Cx\cos(\phi) + Dx^2}, \quad (1)$$

where T is the normal transmittance for the system of thin film on transparent substrate surrounding by air (refractive index = 1), and taking all multiple reflection at the interface [11,25] into account, in case of $k^2 \ll n^2$. $A = 16n^2s$, $B = (n+1)^3(n+s^2)$, $C = 2(n^2-1)(n^2-s^2)$, $D = (n-1)^3(n-s^2)$, $\phi = 4\pi nd/\lambda$, $x = \exp(-\alpha d)$, $k = \alpha\lambda/4\pi$. Here n and s are the refractive indexes of the film and the substrate, d is the thickness of the film and α is the absorption coefficient of the film and λ is the wavelength. The refractive index of the substrate $s = 1/T_s + (1/T_s^2 - 1)^{1/2}$, where T_s is the transmission of the substrate.

Here, the refractive index of the films obey the simple classical dispersion relation for a single oscillator centered at wavelength λ_0 [26] is expressed by

$$n^2 = 1 + \frac{(n_0^2 - 1)\lambda^2}{\lambda^2 - \lambda_0^2},$$

where n_0 is the infinite wavelength refractive index. The wavelength dependence of the absorption process is complicated, therefore, if the total absorption coefficient is small, it may be expanded in a Taylor series around the photon energy far from absorption line. If only terms up to second degree are included (α varies slowly with λ), the relation for α can be written as:

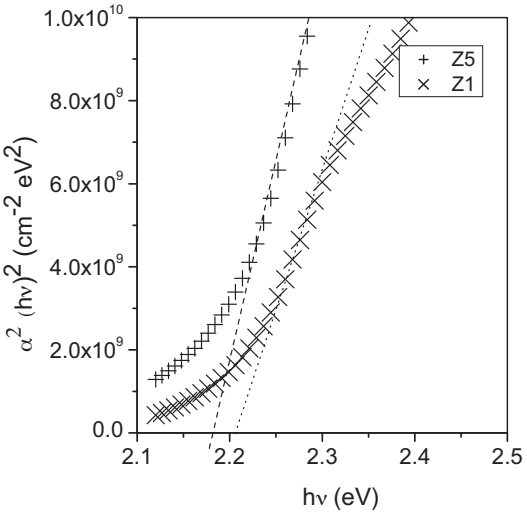

Fig. 4. Plot of (vs. photon energy for Z1 and Z5.

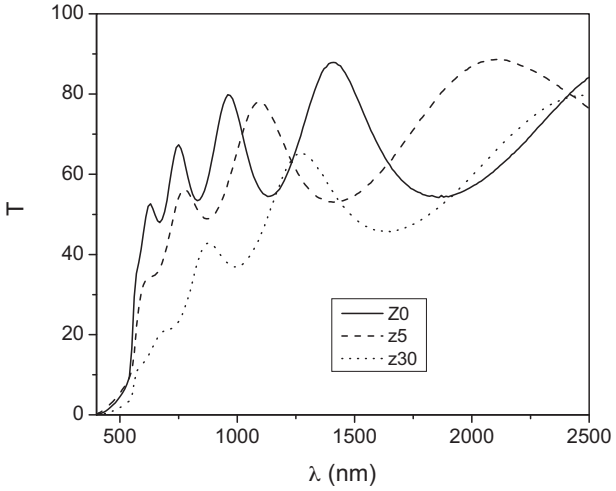

Fig. 6. Transmittance of immersed and heated films.

$\alpha = c + g/\lambda + f/\lambda^2$, where c, g and f are fitting parameters. The values of n and d, obtained by fitting of transmittance data to Eq. (1), were used to calculate α in the high absorption region. The exact solution of Eq. (1) for x is:

$$x = \frac{\left\{\left(C_1 + \frac{A}{T}\right) - \left[\left(C_1 + \frac{A}{T}\right)^2 - 4BD\right]^{1/2}\right\}}{2D}, \quad where\, C_1 = C\cos(\phi).$$

For allowed transition, α varies with photon energy ($h\nu$) as the well-known dependence $\alpha h \sim (h\nu - E_g)^{1/2}$. Near the absorption edge, the optical energy gap (E_g) is obtained by extrapolating $(\alpha h\nu)^2$ against photon energy plot, as shown in Fig. 4. Fig. 5 shows that heating the films in vacuum for 1 h at 400 °C, after immersion, improve the transmittance of the films. This attributed to diffusion of silver into the entire film rather than residing on the film surface. The films transmittance decreases as the immersion time increases (Fig. 6), as result of increasing the silver concentration in the films. Fig. 7 shows a good fitting of the experimental transmission data to Eq. (1). The calculated optical results are listed in Table 2. The refractive index of the films increases as the immersion time increases. Higher Ag concentration in the films leads to higher refractive index and decrease of the optical energy gap. This indicates that high doping occurs, which lead to prominent shift in the optical energy gap (Fig. 8).

3.3. Electrical conductivity

The room temperature resistivities of the films are listed in Table 3. The resistivity of as deposited film is very high (~10^6 (cm) as expected for ZnTe films on amorphous glass substrate [5,6,11]. The resistivity of the films is decreased as function of immersion time, in $AgNO_3$ solution. However increase in the resistivity is observed after heating the immersed film in vacuum (Table 3). This is due to that the electrical contacts, used for measuring the resistivity, were on the films surface where the Ag was concentrated after immersion (ion exchange process occurs at the film surface). Ag diffused in the entire film after heating the immersed films. The p-type conductivities of the films were confirmed by the well-known hot probe method. The dark DC electrical conductivity (() of the films as function of temperature was studied in the temperature range of 30–200 °C. The DC conductivity, in this temperature region, is represented by the following relation [27,28].

$$\sigma = \sigma(0)\exp\left[\frac{-(E_f - E_v)}{kT}\right],$$

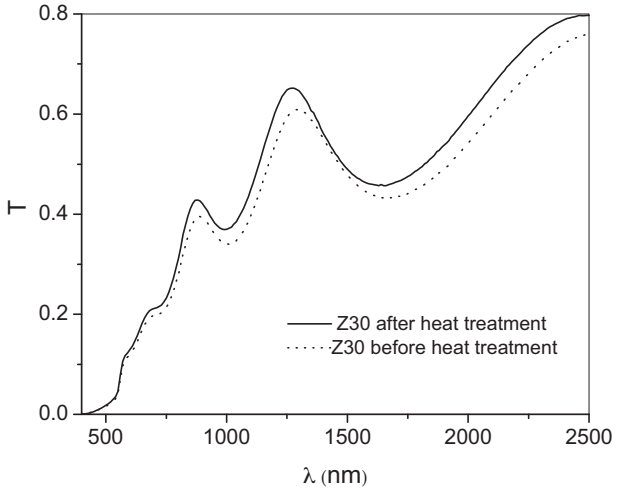

Fig. 5. Transmittance of Z30 before and after heating at 400 °C for 1 h.

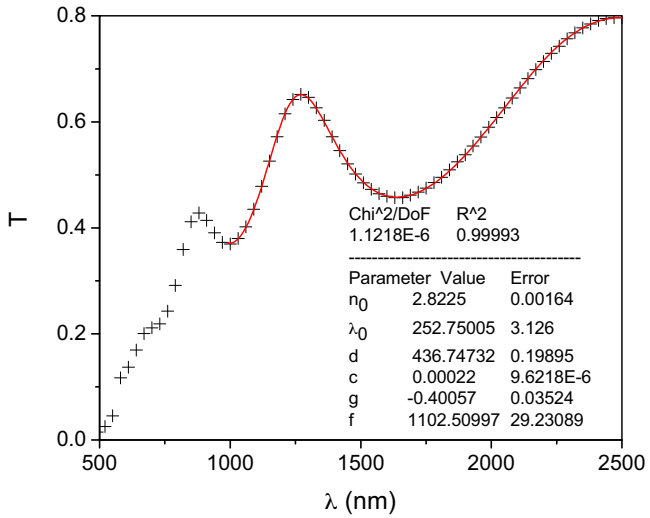

Fig. 7. Transmission data along with fitting to Eq. (1) of heated Z30.

Table 2
Table 3 optical results.

Film number	Thickness (nm)	Refractive index $n = \left(1 + \frac{(n_0^2-1)\lambda^2}{\lambda^2-\lambda_0^2}\right)^{1/2}$		Energy gap (eV)
		n_0	λ_0	
Z0	514	2.71	228	2.24
Z1	477	2.72	268	2.21
Z5	386	2.75	385	2.18
Z30	436	2.82	252	2.16

Table 3
Electrical properties of the films.

Film number	Immersion time (min)	Room temperature resistivity of immersed films (Ω cm)	Room temperature resistivity of heated films (Ω cm)	E_a (eV)
Z0	0	4.5×10^6	4.5×10^6	0.63
Z1	1	1400	8.1×10^3	0.42
Z5	5	18.6	5.9×10^2	0.25
Z30	30	0.052	3.54	0.14
Ag-doped ZnTe by two- source evaporation[a]			$5.5 \times 10^6 - 550$	0.74 – 0.38

[a] Taken from [10].

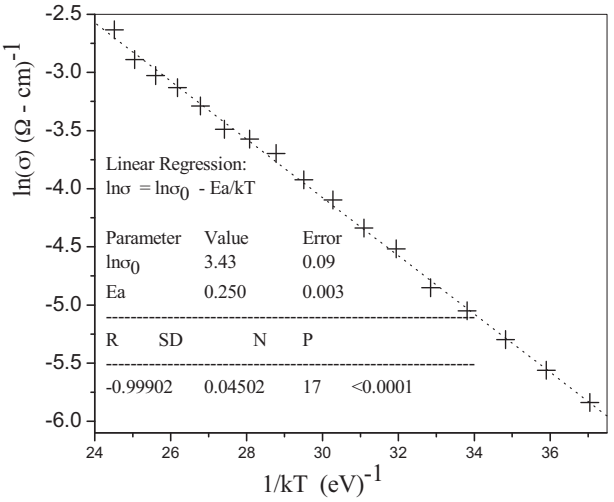

Fig. 8. Fitting of ln(σ) to calculate E_a for heated Z5.

where E_v represents the critical energy at which delocalization of states in the valance band occurs, ((0) is the conductivity at $1/T = 0$ and E_f is the Fermi energy level.

The dark conductivity activation energy ($E_a \equiv E_f - E_v$) obtained from the slope of the fitting $ln(\sigma)$ vs. $1/kT$ plot (Fig. 8). The activation energies of all the film are listed in Table 3. The dark conductivity activation energy of the as-deposited film found to be 0.63 eV, which is close to that mentioned (0.65 eV) in the available literature [27]. The value of activation energy decreases as the immersion time increases, as listed in Table 3. The minimum activation energy belongs to the film which is immersed for 30 min. The decrease of the activation energy indicates an increase in Ag concentration and a strong interaction among the impurities (i.e. shift of E_f closer to the valance band). It is obvious, from Table 3 that the conductivity and the activation energy were lower than that reported for films prepared by two- source evaporation. The comparatively rough surfaces of the films allows more area of the ZnTe films to expose to the solution during ion exchange process, which increase the quantity of Ag ions adsorbed at the film surface.

4. Conclusions

ZnTe thin films are prepared by low-cost simple technique (CSS). Low resistive silver doped films was achieved by an ion exchange process (immersion the post prepared films in $AgNO_3$). All ZnTe films were cubic in structure with [1 1 1] preferred orientation. Small peaks, related to Ag_2Te, appear in the XRD diffraction pattern for of the long time immersed film. The highest conductivity is found to be for the film immersed for 30 min. The surface morphology is almost the same for all films. The films lose their transparency as the immersion time increases. Increase of the films refractive index and shift of optical band gap are also observed. Controlling of immersion time is important parameter to improve the electrical conductivity of the films without drastic change in their optical properties.

References

[1] A. Erlacher, A.R. Lukaszew, H. Jaeger, B. Ullrich, Surface Science 600 (2006) 3762.
[2] K.R. Murali, M. Ziaudeen, N. Jayaprakash, Solid-State Electronics 50 (2006) 1692.
[3] K. Sato, M. Hanafusa, A. Noda, A. Arakawa, M. Uchida, T. Asahi, O. Oda, Journal of Crystal Growth 214–215 (2000) 1080.
[4] L. Feng, L. Wu, Z. Lei, W. Li, Y. Cai, W. Cai, J. Zhang, Q. Luo, B. Li, J. Zheng, Thin Solid Films 515 (2007) 5792.
[5] H. Bellakhder, A. Outzourhit, E.L. Ameziane, Thin Solid Films 382 (2001) 30.
[6] A.M. Salem, T.M. Dahy, Y.A. El-Gendy, Physica B 403 (2008) 3027.
[7] V.S. John, T. Mahalingam, J.P. Chu, Solid-State Electronics 49 (2005) 3.
[8] O. de Melo, E.M. Larramendi, J.M. Duart, M.H. Velez, J. Stangl, H. Sitter, Journal of Crystal Growth 307 (2007) 253.
[9] S.S. Kale, R.S. Mane, H.M. Pathan, A.V. Shaikh, Oh-Shim Joo, S. Han, Applied Surface Science 253 (2007) 4335.
[10] A.K.S. Aqili, A. Maqsood, Z. Ali, Applied Surface Science 191 (2002) 280.
[11] A.K.S. Aqili, Z. Ali, A. Maqsood, Applied Surface Science 167 (2000) 1.
[12] A.A. Ibrahim, Vacuum 81 (2006) 527.
[13] A. Maqsood, M. Shafique, Journal of Material Science 39 (2004) 1101.
[14] A.K.S. Aqili, A. Maqsood, Z. Ali, Applied Surface Science 180 (2001) 73.
[15] J. Pattar, S.N. Sawant, M. Nagaraja, N. Shashank, K.M. Balakrishna, H.M. Mahesh, International Journal of Electrochemical Science 4 (2009) 369.
[16] N.A. Shah, A. Ali, A.K.S. Aqili, A. Maqsood, Journal of Crystal Growth 290 (2006) 452.
[17] N.A. Shah, A. Ali, A. Maqsood, Journal of Non-Crystaline Solid 355 (2009) 1474.
[18] M. Ristova, M. Ristov, Applied Surface Science 181 (2001) 68.
[19] A. Ali, N.A. Shah, A.K.S. Aqili, A. Maqsood, Semiconductor Science and Technology 21 (2006) 1296.
[20] A. Ali, N.A. Shah, A. Maqsood, Solid-State Electronics 52 (2008) 205.
[21] Z. Ali, A.K.S. Aqili, A. Maqsood, S.M.J. Akhtar, Vacuum 80 (2005) 302.

[22] Z. Ali, A.K.S. Aqili, M. Shafique, A. Maqsood, Journal of Non-Crystaline Solids 352 (2006) 409.
[23] H. Wolf, T. Filz, V. Ostheimer, J. Hamann, S. Lany, Journal of Crystal Growth 214/215 (2000) 967.
[24] Chemical Predictor Software Version 3.0, Ivan Kassal, Copyright 1997–1998 Ivan Kassal.
[25] R. Swanepoel, Journal of Physics E: Scientific Instruments 16 (1983) 1214.
[26] A.K. Walton, T.S. Moss, Proceeding of the Physical Society 81 (1963) 509.
[27] J.B. Webb, D.E. Brodie, Canadian Journal of Physics 52 (1974) 2240.
[28] H.M. Brown, D.E. Brodie, Canadian Journal of Physics 50 (1972) 2512.